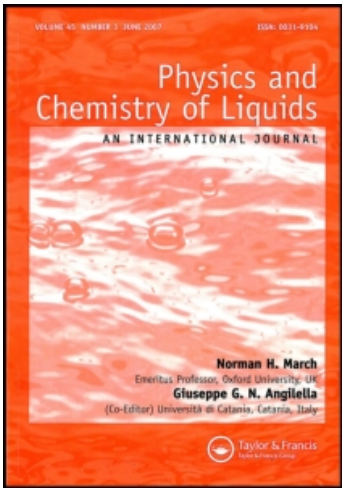

Physics and Chemistry of Liquids
Publication details, including instructions for authors and subscription information:
http://www.informaworld.com/smpp/title~content=t713646857

Optimized cluster theory, optimized random phase approximation and mean spherical model for the square-well fluid with variable range

G. Kahl[a]; J. Hafner[a]
[a] Institut für Theoretische Physik, Technische Universität, Wien, Austria

To cite this Article Kahl, G. and Hafner, J.(1982) 'Optimized cluster theory, optimized random phase approximation and mean spherical model for the square-well fluid with variable range', Physics and Chemistry of Liquids, 12: 2, 109 — 134
To link to this Article: DOI: 10.1080/00319108208084546
URL: http://dx.doi.org/10.1080/00319108208084546

Phys. Chem. Liq., 1982, Vol. 12, pp. 109–134
0031-9104/82/1202-0109$06.50/0

Printed in the U.S.A.

Optimized Cluster Theory, Optimized Random Phase Approximation and Mean Spherical Model for the Square-well Fluid with Variable Range

G. KAHL and J. HAFNER
Institut für Theoretische Physik, Technische Universität, Karlsplatz 13, A 1040 Wien, Austria

(*Received April 30, 1982*)

A critical evaluation of the optimized cluster theory, the optimized random phase approximation and the mean spherical model for describing the effect of attractive forces upon the structure and thermodynamics of liquids is given at the example of the square-well fluid with a variable range of the attractive interaction. Our results demonstrate that for a general width of the attractive well, the optimized cluster theory is more accurate than the mean spherical model.

1 INTRODUCTION

Over the last few years, perturbational methods such as the Gibbs–Bogoljubov variational technique[1,2] and the Weeks–Chandler–Andersen "blip-function" expansion[3–5] have greatly contributed to our understanding of the thermodynamic and structural properties of liquid metals and alloys. The physical picture emerging from these theories is that the liquid has its volume determined by the attractive part of the intermolecular potential, but once the volume has been determined, the liquid may be considered as a hard-sphere fluid confined within that volume. Although this picture is generally correct for simple liquids near their melting point, there are situations, where the attractive part of the interatomic potential becomes more important: (a) in expanded metals, long-wavelength density-fluctuations are observed. These fluctuations cannot be explained in any model considering only repulsive forces and must be attributed to the attractive interactions.[6] (b) In liquid mixtures non-additive attractive interactions cause chemical ordering: if the interaction between two unlike

atoms is more attractive than that between atoms of the same species (i.e. if $\omega_{AB} < \frac{1}{2}(\omega_{AA} + \omega_{BB})$, ω_{ij} is the interaction potential for atoms i and j), heterocoordination will be preferred. If $\omega_{AB} > \frac{1}{2}(\omega_{AA} + \omega_{BB})$, the system will show long-wavelength concentration fluctuations with a tendency towards phase separation[7,8] (see Ref. (9) for the calculation of effective interatomic potentials using pseudo-potential theory and their interrelation with the ordering problem).

The theory needed to describe the influence of the attractive forces on the liquid structure is inherently more complicated than the technique required to reproduce the effect of the repulsion. Andersen and Chandler[10,11] and Andersen *et al.*[12] have proposed a series of related pertubation approximations for describing the effect of attractive interactions on the structure and thermodynamics of liquid and liquid mixtures which they call the optimized random phase approximation (ORPA) and the optimized cluster theory (OCT). Their theory may be cast into the form of a variational problem defining a renormalized ("optimized") potential for the attractive forces. This is a very attractive feature if systems with rather complicated pair potentials—such as liquid metals—are to be considered. In this case, the numerical solution of one of the integral equations relating the pair correlation function to the pair potential is an extremely tricky task, whereas the numerical solution of the variational problem is readily achieved. The ORPA and the OCT have been applied to a variety of potentials, such as the Lennard-Jones potential, simple models of ionic solutions,[13] to mixtures of hard spheres and hard spheres with attractive square well interactions,[14] to a simple square well fluid[15] and to some selected liquid metals.[16,17] The ORPA and the OCT start from an asymptotic form of the direct correlation function for large interparticle separations. Hence they are inherently low-density approximations (although only the OCT becomes exact in the low-density limit). However, the work of Andersen *et al.*[4,13] has shown that at least for moderately strong attractions and relatively elevated temperatures (i.e. for $T^* = (\beta\varepsilon)^{-1} > 0.75$, ε is the depth of the attractive Lennard-Jones interaction, $\beta = 1/k_B T$) the ORPA and especially the OCT are remarkably accurate over the entire range of liquid densities, except for the immediate neighbourhood of the liquid gas coexistence curve. On the other side, the influence of the strength and the range of the attractive interactions on the solutions of the ORPA and the OCT has not been investigated systematically as yet. In view of a prospective application of these theories to liquid metals and alloys near or not too far above their melting point such an investigation seems to be highly desirable, since T^* may be as small as 0.50.

The present study has been performed with intention to fill this gap. ORPA and OCT calculations have been performed for a square-well fluid with varying depth and range of the attractive interaction and for a wide range of

densities and temperatures. The square-well fluid has been chosen as a test system because: (a) it is easy to handle, (b) reasonably well representative for liquid metals and, most importantly, (c) the results of the ORPA and the OCT may be compared with already existing results of computer simulations (Monte-Carlo studies,[18–21] molecular dynamics studies[22,23]) and of analytical calculations (Percus–Yevick (PY) studies,[24–27] hypernetted chain (HNC) studies,[20] mean spherical approximation (MSA),[15] parametric integral equation and perturbation theory: Carley[28,29]) are available for comparison. Our results for the structure and thermodynamics allow for a critical evaluation of the RPA, the ORPA and the OCT (in a variational formulation) for the square-well fluid.

2 SUMMARY OF WELL-KNOWN RESULTS

For a simple fluid of N spherical atoms in a volume V the direct correlation function $c(r)$ is defined by the Ornstein–Zernike (OZ) relation

$$h(r) = c(r) + n \int \mathrm{d}^3 r' c(|\mathbf{r} - \mathbf{r}'|) h(r'). \tag{1}$$

Here $n = N/V$ is the number density, $h(r) = g(r) - 1$ the total correlation function and $g(r)$ the pair correlation function. An approximate integral equation may be derived from the OZ relation by combining it with a closure relating $c(r)$ and $h(r)$. The Percus–Yevick (PY) integral equation is obtained by setting

$$c(r) = f(r) y(r), \tag{2}$$

the hypernetted chain (HNC) approximation is defined by

$$c(r) = f(r) y(r) + y(r) - 1 \ln y(r) - 1 \tag{3}$$

(see Barker and Henderson[30] for a general review of liquid state theory). In Eqs. (2) and (3) $y(r) = g(r) \exp\{\beta u(r)\}$ and $f(r) = \exp\{-\beta u(r)\} - 1$, $u(r)$ is the interatomic potential. For large r, Eq. (2) becomes

$$c(r) = -\beta u(r) \tag{4}$$

This is the random-phase approximation (RPA) which is seen to be the asymptotic form of the PY-closure. Using the RPA-closure not just for large r, but for all r in the attractive region of the potential defines the mean spherical approximation. Hence for a potential with a hard core of diameter

σ, the MSA is specified by

$$c(r) = -\beta u(r) \qquad r > \sigma$$

and

$$h(r) = -1 \qquad r < \sigma \tag{5}$$

combined with the OZ equation. Note that the MSA is identical to the PY equation for the hard sphere fluid.

Let us now turn to systems with a repulsive hard core interaction, i.e.

$$u(r) = u_0(r) + u_1(r) \tag{6}$$

with

$$\begin{aligned} u_0(r) &= \infty \qquad r < \sigma \\ u_0(r) &= 0 \qquad r > \sigma \end{aligned} \tag{7}$$

and an attractive interaction $u_1(r)$. For a square well potential this would be

$$\begin{aligned} &= 0 \qquad && r < \sigma \\ u_1(r) &= -\varepsilon \qquad && \sigma < r < \lambda\sigma \\ &= 0 \qquad && r > \lambda\sigma \end{aligned} \tag{8}$$

The starting approximation for the ORPA and the OCT is to write the direct correlation function as

$$c(r) = c_0(r) + \phi(r) \tag{9}$$

$c_0(r)$ is the direct correlation function of the hard-sphere potential. Outside the core $\phi(r) = -\beta u_1(r)$. Without further specification of $\phi(r < \sigma)$ ($\phi = 0$ or $\phi = -\varepsilon$ are possible choices), this is the RPA for the attractive interaction. It has the unphysical feature of a pair correlation function which is non-zero inside the core. Andersen *et al.*[11] proposed to choose $\phi(r)$ inside the core so that $g(r) = 0$ inside the core. $\phi(r)$ determined by this condition is called the "optimized" potential. If $c_0(r)$ in Eq. (9) is taken to be the analytical solution of the hard-sphere PY-equation,[31,32] this approximation is entirely equivalent to the MSA. If an accurate expression for $c_0(r)$ is used (Andersen *et al.* use the semiempirical $g_0(r)$ of Verlet and Weis[33] and the technique of Grundke and Henderson[34] to construct the corresponding $c_0(r)$), the approximation is called the optimized random phase approximation (ORPA). The ORPA pair correlation is usually written as

$$g(r) = g_0(r) + \mathscr{C}(r) \tag{10}$$

Inserting Eq. (9) in the OZ-relation yields an equation for $\mathscr{C}(r)$ in the form of a chain sum of convolution integrals over the optimized potential $\phi(r)$. The chain may be summed by the standard Fourier transform technique to yield (a caret denotes a Fourier transform of a function)

$$\hat{\mathscr{C}}(k) = \frac{S_0(k)\hat{\phi}(k)S_0(k)}{1 - nS_0(k)\hat{\phi}(k)} \tag{11}$$

Here $S_0(k) = (1 - n\hat{c}_0(k))$ is the static structure factor of the reference system. Note that this is not a solution for $\hat{\mathscr{C}}(k)$ but an integral equation determining the optimized potential ϕ. This integral equation may be solved using a variational procedure.[4] Define the functional F by

$$F(\phi) = \frac{1}{(2\pi)^3 n} \int \mathrm{d}^3k \{nS_0(k)\hat{\phi}(k) - \ln [1 - nS_0(k)\hat{\phi}(k)]\} \tag{12}$$

and take its functional derivative with respect to $\hat{\phi}(k)$

$$\frac{\delta F(\phi)}{\delta \hat{\phi}(k)} = -\frac{n}{(2\pi)^3} \hat{\mathscr{C}}(k) \tag{13}$$

After Fourier-transforming this gives

$$\frac{\delta F(\phi)}{\delta \phi(r)} = -n\mathscr{C}(r) \tag{14}$$

Now since we require $g(r) = 0$ for $r < \sigma$, it follows that

$$\mathscr{C}(r) = 0 \qquad r < \sigma \tag{15}$$

We see that the correct behaviour of the optimized potential is such as to make F stationary with respect to changes in $\phi(r)$ for $r < \sigma$. Note that similar variational formulations may be derived for all the various integral equations derived from the OZ-relation.[3,5]

The ORPA-expression for the free energy A is most easily obtained via the coupling constant formalism, i.e.

$$A = A_0 + \frac{n^2}{2} \int_0^1 \mathrm{d}\lambda \int \mathrm{d}^3r \phi(r) g(r, \lambda) \tag{16}$$

where $g(r, \lambda)$ is the pair correlation function of a system with the attractive interaction $\lambda\phi(r)$. Using (10) and converting the interaction integral to Fourier space allows to carry out the λ − integration with the result

$$A = A_0 - \frac{n^2}{2} \beta \int \mathrm{d}^3r u_1(r) g_0(r) - \frac{1}{2n} F[\phi(r)] \tag{17}$$

Andersen and Chandler[11] have proposed the exponential approximation (EXP)

$$g(r) = g_0(r) \exp\{\mathscr{C}(r)\} \tag{18}$$

for the pair correlation function. The EXP has been derived by rather complicated diagrammatical techniques which need not to be reproduced here. We will present only a very simple argument which should make it at least plausible that the EXP-$g(r)$ can be expected to be more accurate than $g(r)$ calculated using the ORPA. We start from the exact relation (see, e.g. Croxton[36])

$$c(r) = g(r) - 1 - \ln g(r) - \beta u(r) + E(r) \tag{19}$$

A corresponding relation holds for the unperturbed reference system. Here $E(r)$ is a function, the so-called bridge-function, representing the sum of the elementary graphs (or bridge diagrams) in the cluster expansion for the direct correlation function. $E(r) \equiv 0$ defines the HNC closure, cf (3). Very recently, Rosenfeld and Ashcroft[37,38] have shown that within the accuracy of present day computer simulations the bridge function is a universal function, independent of the assumed pair potential. In our case this means $E(r) = E_0(r)$. Thus taking the difference of the relation (19) for the reference system and the perturbed system, we arrive at

$$\ln g(r) - \ln g_0(r) = g(r) - g_0(r) - (C(r) - C_0(r) - \phi(r)) \tag{20}$$

and using (9) and (10) we have finally

$$\ln g(r) = \ln g_0(r) + \mathscr{C}(r) \tag{21}$$

This is just the EXP-result. (20) suggests that the error committed in using the approximate relations (9) and (10) will cancel in the EXP approximation, provided that $g_0(r)$ is the exact hard-core correlation function. The free energy calculated in the same approximation is just the ORPA plus an additional term B_2

$$A = A_{\text{ORPA}} + B_2 \tag{22}$$

$$B_2 = \tfrac{1}{2}n^2 \int \mathrm{d}^3r\{g_0(r)[\exp\{\mathscr{C}(r)\} - \mathscr{C}(r) - 1] - \tfrac{1}{2}\mathscr{C}(r)^2\} \tag{23}$$

(22) is called the ORPA + B_2 approximation. Eq. (22) for the free energy and (18) for the pair correlation function together are referred to as the optimized cluster theory (OCT).

3 VARIATIONAL SOLUTION FOR THE OPTIMIZED POTENTIAL

The optimized potential $\phi(r)$ may be found either by solving the integral equation (11) numerically or by solving the variational condition (14).

Since the functional $F[\phi]$ is positive definite for all ϕ for which the integral exists, the variational condition requires the minimization of $F[\phi]$. This process is straight forward to perform numerically: a simple functional form of $\phi(r)$ containing a finite number of adjustable constants a_i, $i = 1, \ldots, n$ is assumed and the constants are varied to make $F[\phi]$ stationary,

$$\frac{\partial F[\phi(r; a_1, \ldots, a_n)]}{\partial a_i} = 0 \qquad \begin{matrix} r < \sigma \\ i = 1, \ldots, n \end{matrix} \tag{24}$$

In the present work the trial function for the optimized potential is chosen to be

$$\begin{aligned} \phi(r) &= \sum_{n=0}^{m} a_n \left[\frac{1 - r}{\sigma}\right]^n && r < \sigma \\ &= -\beta\varepsilon && \sigma < r < \lambda\sigma \\ &= 0 && r > \lambda\sigma \end{aligned} \tag{25}$$

and the numerical minimization is performed using a gradient routine.[39] It is clear that any finite-order expansion such as (25) spans only a particular subspace and the first task will be to check whether a chosen value of m will be large enough to allow the variational condition $\mathscr{C}(r) = g(r) = 0$ for $r < \sigma$ to be satisfied. The variationally determined $g^{\mathrm{ORPA}}(r)$ for a square well fluid with $\lambda = 1.5$ is shown in Figure 1a for different values of the density n and the strength of the attractive interaction ε for $m = 0$ (this is the RPA) and $m = 2, 4, 6$. The corresponding optimized potential $\phi(r)$ is displayed in Figure 1b.

(We follow the terminology of Andersen *et al.*: MSA means that the reference system is the analytical PY-solution, whereas for ORPA and OCT the reference system is the semi-empirical "exact" $g_0(r)$ of Verlet and Weis together with the Carnahan-Starling[40] expressions for the thermodynamic quantities. In this case $c_0(r)$ is calculated using the technique of Grundke and Hendersen.[34] Throughout this paper the following reduced units will be employed: density $n^* = n\sigma^3$, temperature (depth of square well) $T^* = (\beta\varepsilon)^{-1}$, pressure $P^* = \beta p/n$, internal energy $U^* = 2U\beta/3N$, distance $r^* = r/\sigma$ and wave-vector $q^* = q\sigma$).

We see that even for high densities and strongly attractive interactions $m = 4$ is usually sufficient to satisfy the variational condition (since we require $\phi(r)$ to be continuous for $r = \sigma$, this corresponds to a four-parameter solution). Setting $m = 6$ brings considerably increased numerical difficulties, but only a marginal improvement. Going from $m = 4$ to $m = 6$, the lowering of the value of the functional $F[\phi(r)]$ is only of the order of magnitude of $\sim 0.5\%$ and even considerably smaller in most cases. Therefore a value of

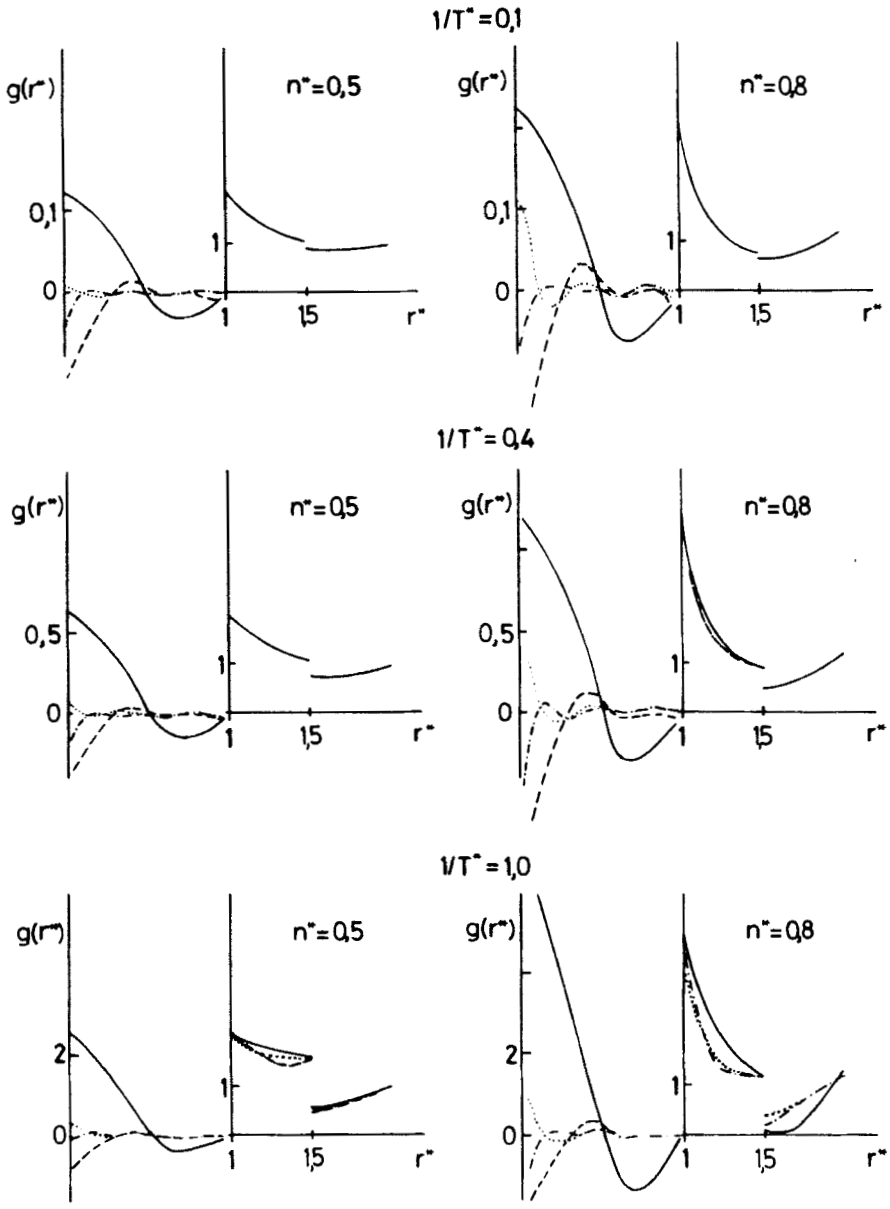

(a)

FIGURE 1 a) Pair correlation function of a square-well fluid with $\lambda = 1.5$, calculated in the ORPA with m variational parameters (see Eq. (24)). Solid line $m = 0$ ($\equiv$RPA), dashed line $m = 2$, dotted line $m = 4$ and dot dashed line $m = 6$. For $1/T^* = 1.0$, the crosses indicate the result of the Monte-Carlo simulation (Ref. 15). b) Optimized potential $\phi(r)$ for a square-well fluid inside the hard core. See Figure 1a.

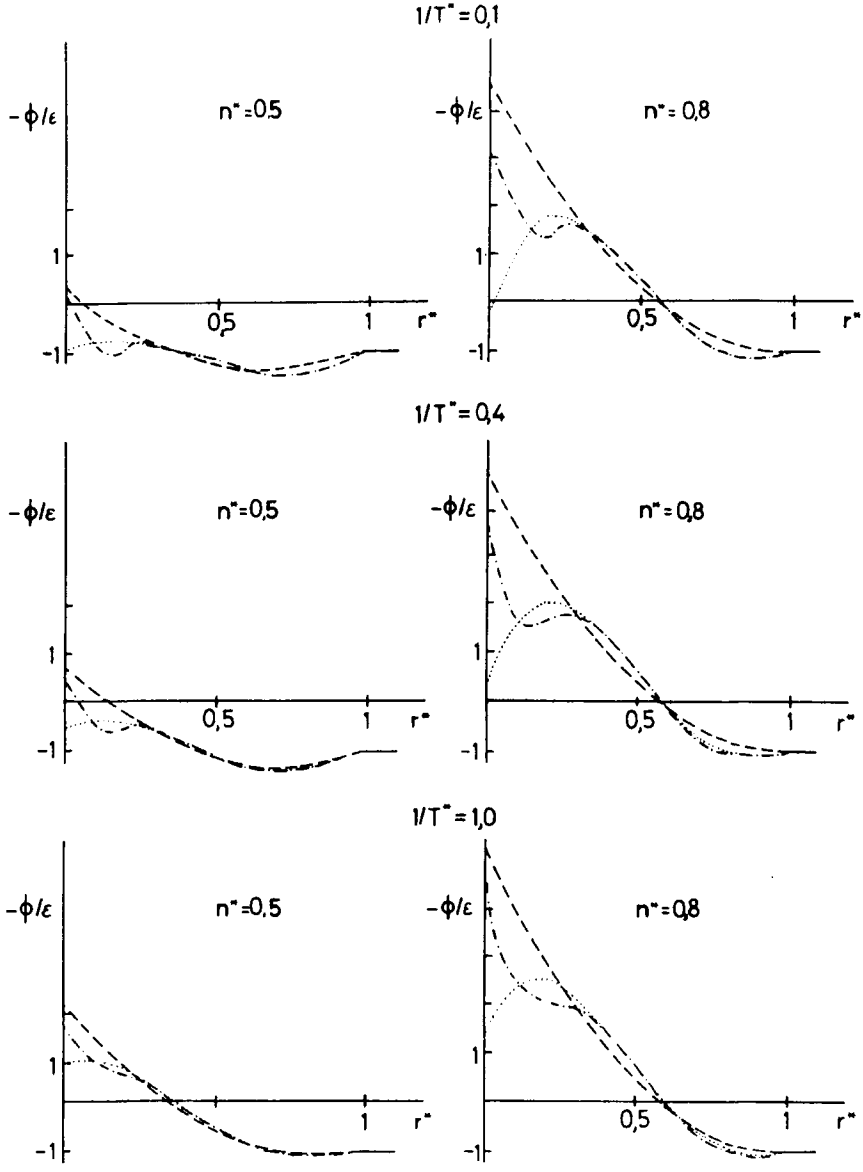

FIGURE 1 (b)

$m = 6$ was considered to be sufficient and no attempt was made to go beyond that.

The minimization of $F[\phi]$ was possible over the entire density range and for square well depths as large as $1/T^* = 1.25$. For more attractive potentials (or lower temperatures) the minimization becomes more difficult (the starting gradients $(\partial F/\partial a_i)_{a_i=0}$ are very large) and the calculation is increasingly time-consuming. However, for $1/T^* > 1.25$ and not too high densities ($n^* < 0.60$) we are already in the coexistence region of the (p, T) phase diagram. Hence, the minimization may be very conveniently performed for the entire liquid region.

A further possibility to check the accuracy of the variational solution of the MSA is to compare it with the integral equation-solution of Smith *et al.*[15] This is done in Table I. It is shown that even for a rather restricted set of variational parameters the variational result converges very well towards the result obtained by solving the MSA integral-equation. Only for the lowest temperatures a six-parameter minimization is really required, for higher temperatures (weaker potentials), a four parameter calculation is usually entirely sufficient.

TABLE I

Comparison of thermodynamic quantities calculated using the variational and the integral-equation formulation of the MSA: internal energy U^* (computed from the energy equation), pressure P^* (computed from the virial equation). The first four lines give the variational result (m is the number of parameters, $m = 0$ is equivalent to the RPA), the fifth line the result obtained by solving the MSA-integral equation (taken from Ref. 15). $n^* = 0.5$

$1/T^*$	U^*	P^*	m
	0.7228	2.8172	0
	0.7741	2.8052	2
0.1	0.7742	2.8033	4
	0.7743	2.8022	6
	0.7741	2.8009	
	−1.8908	−0.7372	0
	−1.6610	−0.6065	2
1.0	−1.6651	−0.5988	4
	−1.6691	−0.6047	6
	−1.6792	−0.6023	

4 STRUCTURE AND THERMODYNAMICS OF THE SQUARE-WELL FLUID WITH $\lambda = 1.5$

We turn now to the discussion of the results obtained by using the MSA, ORPA and OCT for a calculation of the structure and thermodynamics of a square-well fluid with $\lambda = 1.5$ (the influence of a variable range of the attractive potential will be discussed further below).

The pair correlation function $g(r)$ is plotted in Figures 2 to 4 for a series of different densities and pressures. The comparison with the Monte-Carlo computer simulations[15] shows $g_{\mathrm{MSA}}(r)$ to be remarkably accurate, except for $r^* \gtrsim \lambda$ and high densities and low temperatures, where $g_{\mathrm{MSA}}(r)$ is too low. $g_{\mathrm{ORPA}}(r)$ is seen to be no improvement over $g_{\mathrm{MSA}}(r)$: $g_{\mathrm{ORPA}}(r)$ is invariably too high at contact ($r^* = 1$) and it shares the deficiency of $g_{\mathrm{MSA}}(r)$ near $r^* \gtrsim \lambda$. The exponential approximation $g_{\mathrm{EXP}}(r)$ is more accurate at contact, but for low densities and temperatures, $g_{\mathrm{EXP}}(r)$ is too high at both sides of the discontinuity at $r^* = \lambda$. A better overall agreement is obtained with the linearized version of the exponential approximation (LEXP), proposed by Verlet and Weis[41]

$$g_{\mathrm{LEXP}}(r) = g_0(r)(1 + \mathscr{C}(r)) \tag{26}$$

but only for $r^* \gtrsim \lambda$ LEXP is really superior to the MSA. However, it should not be overlooked that the good agreement obtained with the MSA is at least to some degree fortuitous: both $g_0(r)$ and $\mathscr{C}_{\mathrm{MSA}}(r)$ are too small individually and there is an appreciable cancellation of errors.

The static structure factor for a square-well fluid with $\lambda = 1.5$ calculated using the RPA and the ORPA is shown in Figure 5. The optimization strongly reduces the magnitude of the first peak. The comparison with the hard-sphere structure factor $S_0(q)$ shows that the optimization tends to reduce the influence of the attractive forces on the structure of the liquid. The density-dependence of the ORPA square-well structure factor is shown in Figure 6. $S(q)$ is seen to be strongly damped with decreasing density. The most important effect of the attractive interactions is to enhance the low-q limit of $S(q)$ compared to the sphere fluid: at $n^* = 0.1$ $S^{\mathrm{ORPA}}(0) = 1.04$ for $1/T^* = 0.5$ compared to $S_0(0) = 0.66$.

There are several routes from the pair correlation function to the thermodynamic quantities: the energy U^* may be calculated using the energy equation

$$U^* = 1 - \frac{4\pi}{3}\frac{n^*}{T^*}\int_1^\lambda g(r^*)r^{*2}\,\mathrm{d}r^* \tag{27}$$

or by numerically differentiating the free energy with respect to the temperature.

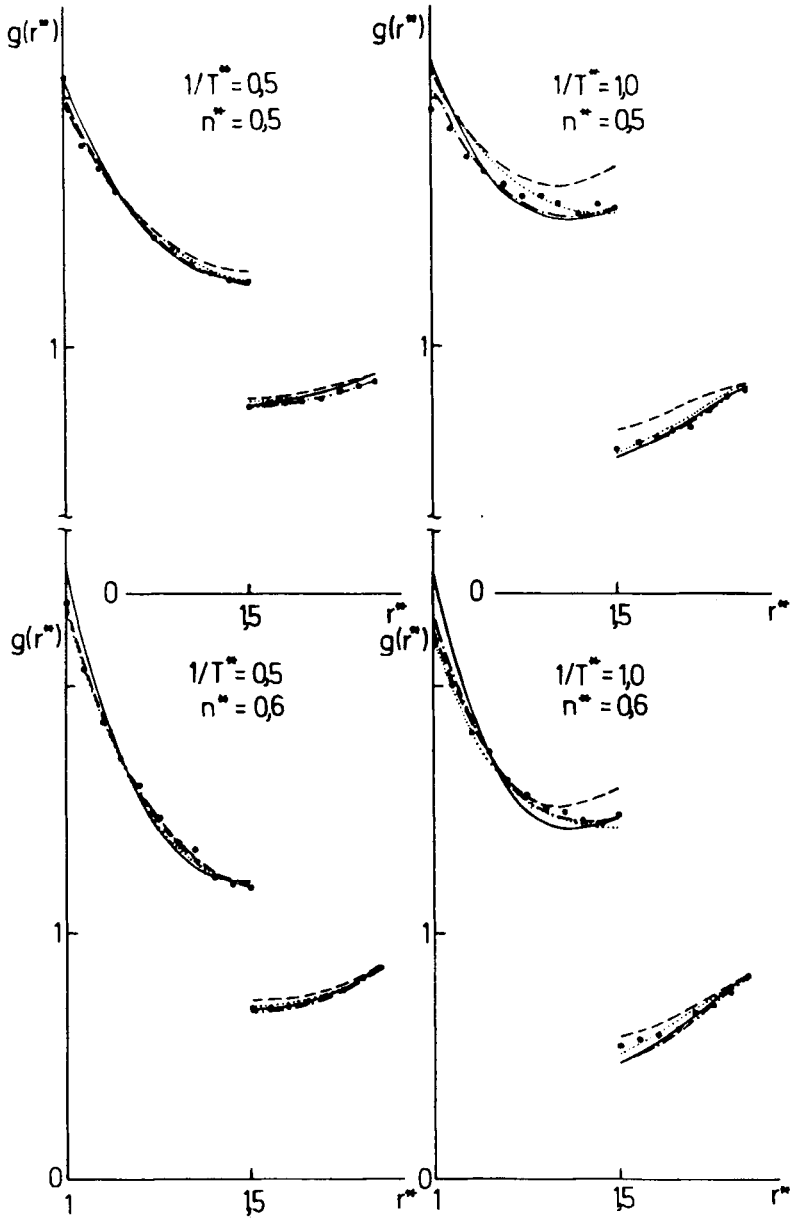

FIGURE 2 Pair correlation function $g(r)$ for the square-well fluid with $\lambda = 1.5$, calculated in the MSA, ORPA, EXP and LEXP approximations for different densities and temperatures. The solid circles represent the result of the Monte-Carlo calculation of Henderson *et al.*,[20] solid line ORPA, dashed line EXP, dotted line LEXP, dot dashed line MSA.

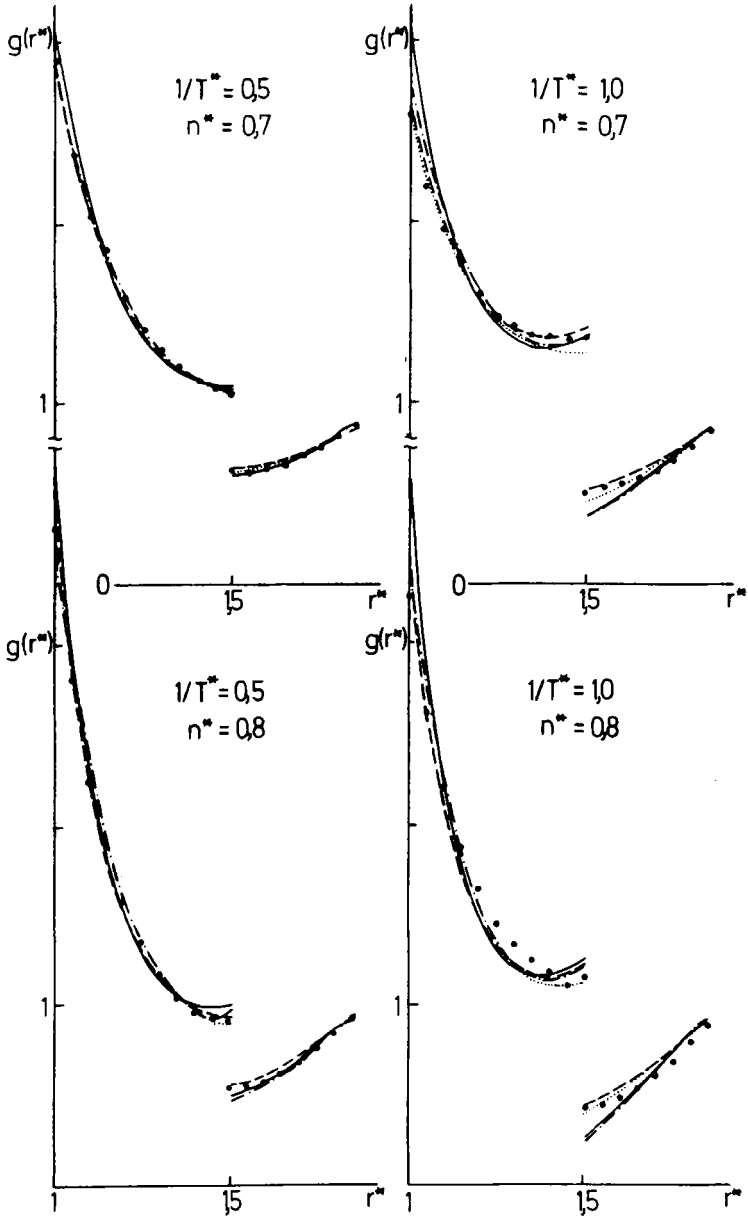

FIGURE 3 See Figure 2.

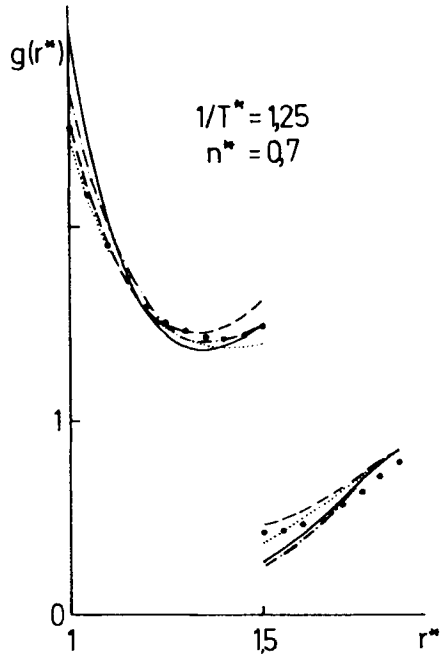

FIGURE 4 See Figure 2.

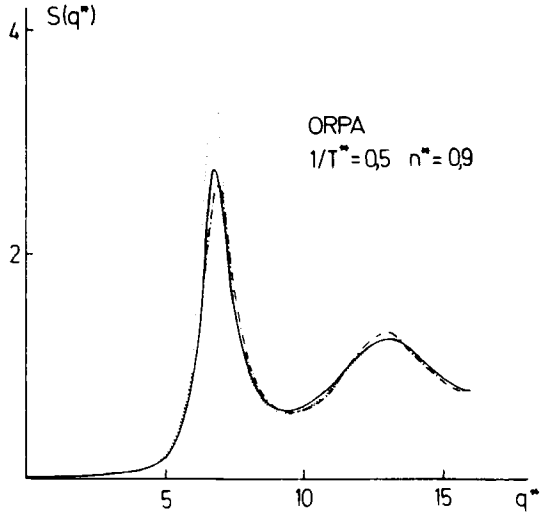

FIGURE 5 Static structure factor for the square-well fluid with $\lambda = 1.5$, calculated in the RPA (dotted line) and in the ORPA (full line), and for a hard sphere fluid of same density (dot dashed line).

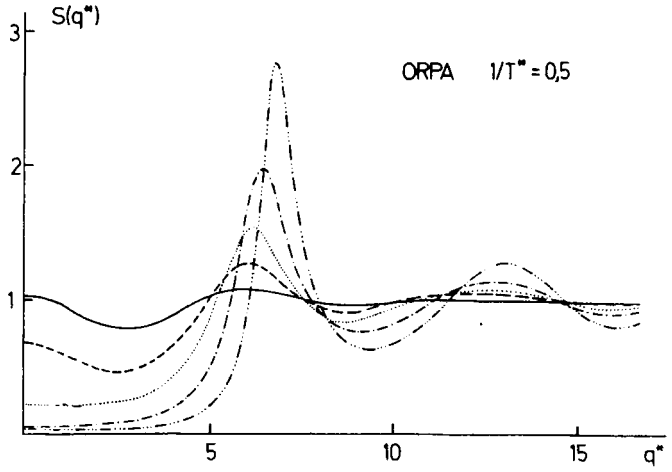

FIGURE 6 Density dependence of the static structure factor of the square-well fluid in the ORPA: — $n^* = 0.1$, - - - - $n^* = 0.3$, ... $n^* = 0.5$, —— $n^* = 0.7$, — · — $n^* = 0.9$.

The pressure can be calculated from the virial equation

$$P^* = 1 - \frac{4\pi}{3}\beta n\sigma^3 \int_0^\infty \frac{du(r^*)}{dr^*}\, g(r^*) r^{*3}\, dr^* \tag{28}$$

Eq. (28) has to be handled with some care because both $u(r^*)$ and $g(r^*)$ are discontinuous at $r^* = 1$ and $r^* = \lambda$. The integrand may be rewritten as $\beta g(r)(du(r)/dr) = y(r)(de(r)/dr)$ ($e(r)$ standing for $\exp(-\beta u(r))$), and if $y(r)$ is continuous (EXP), the integral may be conveniently calculated in this form giving[15]

$$P^* = 1 + \frac{2\pi}{3} n^* \{g(\sigma_+) - \lambda^3 (g(\lambda\sigma_-) - g(\lambda\sigma_+))\} \tag{29}$$

For the MSA, ORPA and LEXP approximations $y(r)$ is discontinuous for $r^* = \lambda$. Smith *et al.*[15] have shown that the pressure equation may be written as

$$P^* = 1 + \frac{2\pi}{3} n^* \left\{ g(\sigma_+) - \frac{\lambda^3}{2T^*} (g(\lambda\sigma_-) + g(\lambda\sigma_+)) \right\} \tag{30}$$

A second way to calculate the pressure is to integrate U/T with respect to the temperature to obtain the free energy A and then to differentiate A numerically with respect to n to obtain the pressure. For the MSA and the ORPA this is performed analytically to yield[15]

$$P^* = P_0^* + \frac{\pi}{3} n^* \left[g^2(\sigma_+) - g_0^2(\sigma_+) - \frac{\lambda^3}{T^*} (g(\lambda\sigma_-) + g(\lambda\sigma_+)) \right] \tag{31}$$

where g_0 and P_0^* are the hard-sphere correlation function and pressure, the latter being given by the Carnahan–Starling[40] expression. For the OCT (=ORPA + B_2) and LEXP approximations an analytical calculation is not possible and the energy-equation-pressure must be calculated by differentiating the free energy A (given by eqs. (22),(23)) numerically with respect to density.

A third way to the equation of state is the compressibility equation relating the isothermal compressibility χ_T to the long-wave length limit of the static structure factor

$$\frac{\beta}{n}\chi_T^{-1} = \beta\left(\frac{\partial p}{\partial n}\right)_T = P^* + n^*\left(\frac{\partial P^*}{\partial n^*}\right)_T = 1 - \hat{c}(0) = S(0)^{-1} \qquad (32)$$

In Table II the internal energies are compiled and compared with the

TABLE II

Reduced internal energy U^* for the square-well fluid with $\lambda = 1.5$, calculated using the energy equation for the MSA, ORPA, OCT (=EXP) and LEXP approximations and compared with the Monte Carlo (MC) results of Ref. 20

	n^*				
	0.5	0.6	0.7	0.8	
$1/T^*$					
	0.421	0.289	0.159	0.043	MSA
	0.421	0.291	0.164	0.048	ORPA
0.25	0.418	0.292	0.171	0.061	EXP
	0.420	0.294	0.172	0.062	LEXP
	0.420	0.289	0.162	0.045	MC
	−0.209	−0.475	−0.733	−0.962	MSA
	−0.210	−0.469	−0.724	−0.956	ORPA
0.50	−0.233	−0.474	−0.708	−0.908	EXP
	−0.220	−0.461	−0.695	−0.897	LEXP
	−0.212	−0.472	−0.705	−0.954	MC
	−0.905	−1.293	−1.680	−2.028	MSA
	−0.906	−1.289	−1.668	−1.987	ORPA
0.75	−0.981	−1.322	−1.648	−1.937	EXP
	−0.935	−1.276	−1.604	−1.842	LEXP
	−0.946	−1.293	−1.676	−1.996	MC
	−1.665	−2.156	−2.664	−3.126	MSA
	−1.676	−2.151	−2.650	−3.114	ORPA
1.00	−1.865	−2.245	−2.646	−2.999	EXP
	−1.747	−2.137	−2.540	−2.903	LEXP
	−1.713	−2.183	−2.658	−3.125	MC
			−3.700	−4.276	MSA
			−3.675	−4.275	ORPA
1.25			−3.709	−4.148	EXP
			−3.498	−3.957	LEXP
			−3.675	−4.252	MC

results of the computer experiment. The predictions of the MSA and the ORPA are remarkably accurate over the entire range of temperatures and pressures. Generally the difference between theory and computer experiment is smaller than two percent, i.e. smaller than the statistical inaccuracy of the computer simulation. The EXP and LEXP approximations are appreciably worse than the MSA and ORPA results.

The corresponding results for the pressure are given in Table III. In the MSA the pressures calculated via the energy equation are in good agreement

TABLE III

Reduced pressure P^* for the square-well fluid with $\lambda = 1.5$, calculated using the virial equation in the MSA, ORPA, OCT (=EXP) and LEXP approximations. For the MSA the pressure calculated using the energy equation is given as well. The Monte Carlo results of Ref. 20 are given for comparison.

	n^*				
$1/T^*$	0.5	0.6	0.7	0.8	
	2.24	3.03	4.21	5.93	MSA-V
	2.28	3.11	4.43	6.49	MSA-E
	2.34	3.24	4.62	6.71	ORPA
0.25	2.29	3.12	4.43	6.48	EXP
	2.29	3.13	4.43	6.48	LEXP
	2.31	3.13	4.49	6.47	MC
	1.29	1.91	3.09	4.83	MSA-V
	1.30	1.97	3.19	5.29	MSA-E
	1.42	2.17	3.49	5.58	ORPA
0.50	1.32	1.96	3.16	5.17	EXP
	1.33	1.94	3.15	5.16	LEXP
	1.35	1.97	3.20	5.08	MC
	0.34	0.85	1.94	3.73	MSA-V
	0.35	0.96	1.92	4.01	MSA-E
	0.47	1.08	2.34	4.38	ORPA
0.75	0.33	0.74	1.84	3.73	EXP
	0.39	0.78	1.86	3.74	LEXP
	0.46	0.70	1.82	3.84	MC
	−0.59	−0.25	0.79	2.64	MSA-V
	−0.56	−0.37	0.66	2.84	MSA-E
	−0.46	0.01	1.17	3.28	ORPA
1.00	−0.63	−0.43	0.50	2.49	EXP
	−0.48	−0.32	0.58	2.57	LEXP
	−0.45	−0.21	0.59	2.34	MC
			−0.32	1.52	MSA-V
			−0.67	1.63	MSA-E
			−0.04	2.12	ORPA
1.25			−0.95	2.14	EXP
			−0.76	1.31	LEXP
			−0.54	1.35	MC

with experiment, much better than those calculated from the virial equation. The discrepancy between the two pressures is a measure for the internal inconsistency of a theory. In the case of the MSA the difference is quite large, especially for high densities and high temperatures. In the case of the OCT the consistency check is more difficult to perform: we have to compare the pressure P_V^* calculated from the virial equation (29) and the $g(r^*)$ ORPA-EXP with the pressure P_A^* obtained by numerically differentiating the free energy computed in the ORPA + B_2 (21,22) with respect to density. For the energy this means that U_E^* calculated from Eq. (27) (and ORPA-EXP for $g(r)$) is compared with U_A^* obtained by numerically differentiating A/T computed as ORPA + B_2) with respect to T. The consistency check for the OCT is presented in Table IV. The OCT satisfies the required consistency very well for the case of the internal energy and even for the pressure the OCT is found to be somewhat better consistent than the MSA. The MSA-energy-equation P^* and the EXP and LEXP virial-equation pressures show the best agreement with the computer experiment, for strongly attractive potentials the LEXP and MSA-E pressures are more accurate than the EXP-result.

Smith and co-workers[15] have shown that for the square-well fluid the MSA is definitely superior to PY and HNC theories. Our work demonstrates that

TABLE IV

Comparison of the OCT values for U_E^* and P_V^* derived from the energy and virial equations respectively and by differentiating the ORPA + B_2 free energy (U_A^*, P_A^*).

	n^*							
	0.2		0.4		0.6		0.8	
$1/T^*$	U_A^*	U_E^*	U_A^*	U_E^*	U_A^*	U_E^*	U_A^*	U_E^*
0.1	0.920	0.920	0.826	0.825	0.723	0.723	0.626	0.627
0.2	0.831	0.830	0.643	0.640	0.437	0.437	0.246	0.250
0.3	0.732	0.730	0.451	0.444	0.145	0.144	−0.141	−0.131
0.4	0.621	0.616	0.248	0.234	−0.156	−0.159	−0.534	−0.517

	n^*					
	0.3		0.5		0.7	
$1/T^*$	P_A^*	P_V^*	P_A^*	P_V^*	P_A^*	P_V^*
0.0	2.01	1.75	3.29	3.17	5.77	5.32
0.1	1.80	1.76	2.91	2.88	5.26	5.22
0.2	1.59	1.54	2.52	2.49	4.76	4.69
0.3	1.38	1.33	2.14	2.10	4.25	4.17
0.4	1.17	1.11	1.76	1.70	3.76	3.68
0.5	0.96	0.89	1.38	1.32	3.26	3.16

TABLE V

Compressibility factors $\beta(\partial p/\partial n)_T$ for the square-well fluid with $\lambda = 1.5$ in the MSA, ORPA and OCT, calculated using the compressibility equation (C) and by numerically differentiating the virial (V) and energy-equation (E) pressures. The density is $n^* = 0.8$

	MSA			ORPA		OCT
$1/T^*$	(C)	(V)	(E)	(C)	(V)	(V)
0.1	28.66	22.91	27.28	27.85	27.47	27.42
0.2	27.62	22.44	27.10	26.88	27.23	27.11
0.25	27.17	22.36	27.04	26.25	27.09	26.95
0.3	26.67	22.25	26.70	25.71	26.97	26.80
0.4	25.70	22.09	26.77	24.57	26.75	26.70
0.5	24.75	22.07	26.60	23.47	26.27	26.35

the OCT is more accurate than the PY and HNC approximations, but not really superior to the MSA: the OCT gives better results for $g(r)$, is of comparable accuracy for the pressure, but less accurate for the internal energy.

The inverse compressibility factor $\beta(\partial p/\partial n)_T = S(0)^{-1}$ calculated from the compressibility equation (32) and by numerically differentiating the virial- and energy equation pressures is given in Table V for the MSA, ORPA and OCT. Again the ORPA satisfies the compressibility check somewhat better than the MSA. The OCT compressibility calculated from the virial equation differs only very little from the corresponding ORPA-value.

These remarks apply only to the special case of $\lambda = 1.5$. The more general case of a variable width of the attractive well is considered in the following section.

5 STRUCTURE AND THERMODYNAMICS OF A SQUARE-WELL FLUID WITH A VARIABLE RANGE OF INTERACTION

Most of the results presented up to now in the literature refer to a square-well fluid with $\lambda = 1.5$. This choice of the range of interaction is a very special one, since the outer limit of the attractive potential is made to agree with the first minimum of the pair correlation function of the unperturbed hard-sphere fluid. Only a very few results for $\lambda \neq 1.5$ have been published: Rosenfeld and Thieberger[21] presented Monte-Carlo simulations for $\lambda = 1.2042$ and $\lambda = 1.3675$ in the density range $0.202 \leq n^* \leq 0.707$ and in the inverse temperature range $0 \leq 1/T^* \leq 1.0$, Tago[26] has solved the PY-equation for $\lambda = 1.85$, but no systematic investigation of the influence of the interaction range upon the properties of the square-well fluid has been attempted as yet.

In Figures 7 and 8 we show the pair correlation function of a square-well fluid with $n^* = 0.8$ and $1/T^* = 0.25$ with λ varying between 1.2 and 1.7,

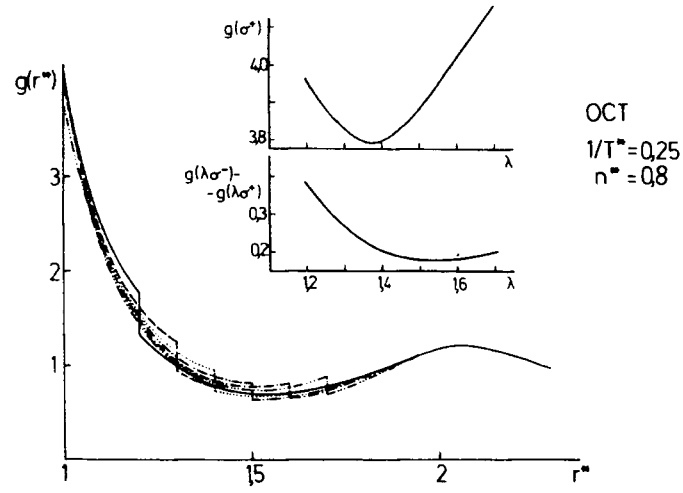

FIGURE 7 Pair correlation functions of a square-well fluid at $n^* = 0.8$, $1/T^* = 0.25$ as a function of the range of the attractive interaction ($\lambda = 1.2$ to 1.7), calculated in the OCT. The variation of the contact-value $g(\sigma_+)$ and of the discontinuity $g(\lambda\sigma_-) - g(\lambda\sigma_+)$ with λ is shown in the inset. $\lambda = 1.2$: —; $\lambda = 1.3$: — —; $\lambda = 1.4$: · · · ·; $\lambda = 1.5$: — · —; $\lambda = 1.6$: — — —: $\lambda = 1.7$: — · · —.

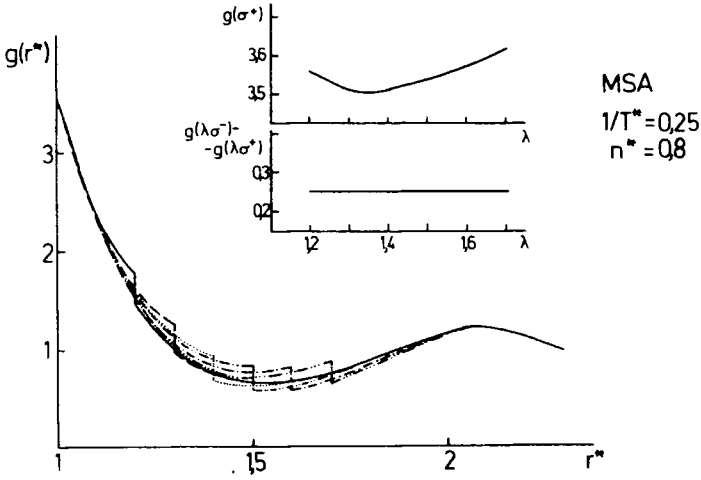

FIGURE 8 As Figure 7, but MSA-results.

calculated in the MSA and OCT. The remarkable difference is that for $\lambda > 1.5$ the $g(r)$ has a minimum in the range $\sigma < r < \lambda\sigma$, but not for $\lambda \leq 1.5$. The region around $r \sim 1.5\sigma$ is a geometrically excluded region for packing reasons. That a minimum in $g(r)$ exists in the attractive square-well fluid indicates that the attractive forces are not strong enough to fill the geometrically excluded regions. It is also interesting to observe the variation of the value of $g(r)$ at contact ($g(\sigma_+)$) and at both sides of the discontinuity ($g(\lambda\sigma_-)$, $g(\lambda\sigma_+)$) with λ. For both OCT and MSA $g(\sigma_+)$ shows a distinct minimum close to $\lambda = 1.4$. The existence of this minimum is a consequence of the interference between attractive and repulsive forces: the attractive forces tend to fill the attractive well more or less uniformly. If $(\lambda - 1)$ is sufficiently small, the action of the attractive forces is not hindered by the repulsions, $g(\sigma_+)$ decreases as the attractive region is expanded. However, if $\lambda \geq 1.5$, parts of the attractive region are at the same time geometrically forbidden. The attractive forces still tend to fill the attractive well, but because of the repulsive forces the particles are pushed to the inner and to the outer boundary of the well. Note that the variation of $g(\sigma_+)$ with λ is distinctly stronger in the MSA.

In the MSA, the size of the jump discontinuity in $g(r)$ is by definition constant, $g(\lambda\sigma_-) - g(\lambda\sigma_+) = 1/T^* = \beta\varepsilon$. In the OCT we have

$$g(\lambda\sigma_-) - g(\lambda\sigma_+) = g_0(\lambda\sigma)e^{\varphi(\lambda\sigma-)}(1 - e^{-\beta\varepsilon}). \tag{33}$$

The first two factors vary with λ: because of the first factor, the size of the discontinuity tends to follow the oscillations of the hard-sphere correlation function, the exponential factor tends widen the gap for small λ's.

The characteristically different behaviour of $(g(\lambda\sigma_-) - g(\lambda\sigma_+))$ in the MSA and in the OCT is also reflected in the thermodynamic properties. Characteristic examples for the variation of the reduced internal energy U^* and the pressure P^* with the range of interaction are shown in Figures 9 and 10. For some selected, but still representative values of the density n^* and the temperature T^*, the combined Monte-Carlo simulation results of Rosenfeld and Thieberger[21] and of Henderson *et al.*[20] allow for a critical evaluation of the accuracy of the analytical theories. This is presented in Tables VI and VII.

The results for the internal energy will be discussed first. According to Eq. (27) we expect that U^* will decrease with increasing λ and that this variation will be stronger at higher densities. Figure 9 displays the expected behaviour and shows that the $U^* = U^*(\lambda)$ relation is approximately linear. The comparison with the Monte-Carlo results is more informative. For $\lambda = 1.5$ we had to note that the MSA is more accurate than the OCT for a calculation of the internal energy, but as for the $g(r)$ it must be remarked that good agreement achieved with the MSA is some degree fortuitous, being due to a cancellation of errors. The new results for smaller λ show that this is true

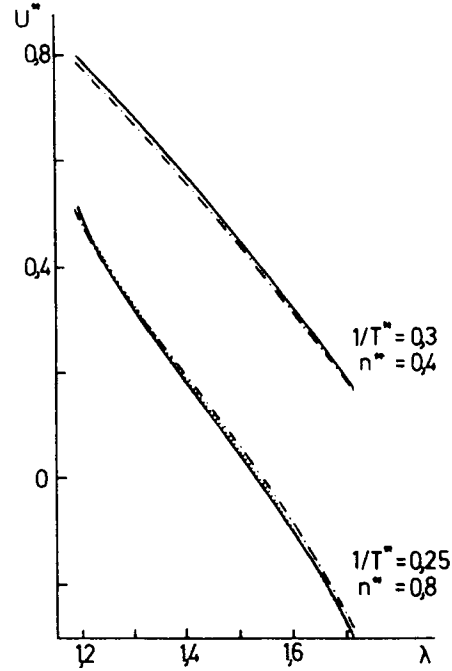

FIGURE 9 Internal energy U^* of a square-well fluid as a function of range of interaction (λ) for two different sets of (T^*, n^*) in the MSA (solid line), ORPA (dotted line) and OCT (dot-dashed line).

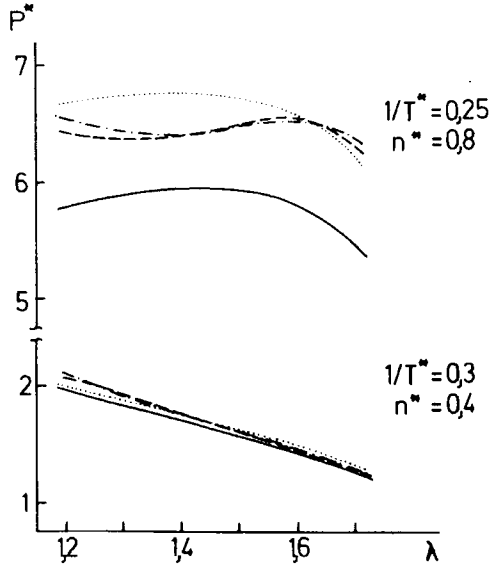

FIGURE 10 Pressure P^* of a square-well fluid as a function of range of interaction (λ) for two different sets of (T^*, n^*): MSA (virial equation): solid line, MSA (energy equation): dashed line, ORPA (virial equation): dotted line, OCT (virial equation): dot-dashed line.

TABLE VI

Reduced internal energy U^* for the square-well fluid with variable λ, calculated using the energy equation for the MSA, ORPA, OCT (=EXP) and LEXP approximations and compared with the Monte Carlo (MC) results of Refs. 20 and 21.

	$\lambda = 1.2042$		$\lambda = 1.3675$		$\lambda = 1.5$		
$1/T^*$	n^*	U^*	n^*	U^*	n^*	U^*	
0.25	0.7071	0.596	0.7071	0.346	0.70	0.159	MSA
		0.592		0.351		0.164	ORPA
		0.579		0.349		0.171	EXP
		0.580		0.351		0.172	LEXP
		0.584[a]		0.331[a]		0.162[b]	MC
0.50	0.4714	0.542	0.4714	0.187	0.50	−0.209	MSA
		0.536		0.184		−0.210	ORPA
		0.486		0.144		−0.233	EXP
		0.498		0.155		−0.220	LEXP
		0.498[a]		0.149[a]		−0.212[b]	MC
1.00	0.4714	−0.038	0.4714	−0.820	0.50	−1.665	MSA
		−0.053		−0.831		−1.676	ORPA
		−0.333		−1.083		−1.865	EXP
		−0.213		−0.968		−1.747	LEXP
		−0.233[a]		−0.966[a]		−1.713[b]	MC
0.25	0.3536	0.855	0.3536	0.729			
		0.854		0.727			
		0.846		0.720			
		0.847		0.721			
		0.843[a]		0.717[a]			

[a] According to Ref. 21.
[b] According to Ref. 20.

indeed the cancellation of errors works only for $\lambda = 1.5$, for smaller λ the OCT and the LEXP yield more accurate internal energies at all densities and temperatures.

The variation of the pressure with the range of interaction is more complicated. The reduced pressure consist (except for the constant ideal-gas contribution) of a positive contribution depending on the value of the pair correlation function at contact and a negative contribution proportional to the gap in $g(r)$ at $r = \lambda\sigma$ (see Eqs. (29) to (31)). The negative term is proportional to λ^3 and for not too high density ($n^* < 0.8$) and low temperatures this term dominates, yielding a decreasing P^* with increasing λ. However, as the gap in $g(r)$ either decreases (EXP-virial-equation) or is modulated with the function $(g(\lambda\sigma_+) + g(\lambda\sigma_-))$ (MSA, ORPA virial and energy equations), the decrease of P^* is only approximately linear with λ for $\lambda \leq 1.6$, but steeper for $1.7 \leq \lambda \leq 2.0$. (Figure 10). Things are more complicated at high densities and temperatures where the positive contribution to the pressure dominates

TABLE VII

Reduced pressure P^* for the square-well fluid with variable λ, calculated using the virial equation in the MSA, ORPA, OCT (=EXP) and LEXP approximations. For the MSA the pressure calculated using the energy equation (MSA-E) is given as well. Monte Carlo simulation results are shown for comparison.

	$\lambda = 1.2042$		$\lambda = 1.3675$		$\lambda = 1.5$		
$1/T^*$	n^*	P^*	n^*	P^*	n^*	P^*	
0.25	0.7071	4.40	0.7071	4.36	0.70	4.21	MSA-V
		4.79		4.57		4.43	MSA-E
		4.89		4.82		4.62	ORPA
		4.88		4.60		4.43	EXP
		4.88		4.59		4.43	LEXP
		4.81 ± 0.20		4.31 ± 0.13		4.49	MC[a]
0.50	0.4714	1.84	0.4714	1.47	0.50	1.29	MSA-V
		2.07		1.54		1.30	MSA-E
		1.92		1.57		1.42	ORPA
		2.09		1.56		1.32	EXP
		2.07		1.58		1.33	LEXP
		2.09 ± 0.09		1.59 ± 0.09		1.35	MC[a]
1.00	0.4714	0.63	0.4714	−0.05	0.50	−0.59	MSA-V
		1.10		0.11		−0.56	MSA-E
		0.73		0.07		−0.46	ORPA
		1.04		0.02		−0.63	EXP
		1.03		0.15		−0.48	LEXP
		0.90 ± 0.12		0.05 ± 0.24		−0.45	MC[a]
0.25	0.3536	1.87	0.3536	1.70			MSA-V
		1.95		1.75			MSA-E
		1.89		1.73			ORPA
		1.96		1.75			EXP
		1.95		1.75			LEXP
		1.92 ± 0.05		1.80 ± 0.08			MC[a]

[a] MC results according to Ref. 21 for $\lambda = 1.2042$ and $\lambda = 1.3675$ and after Ref. 20 for $\lambda = 1.5$.

and $g(\sigma_+)$ shows a rather strong dependence on λ. In this region P^* shows a non- monotonous dependence on λ, whose details can be traced back to the λ-dependence of $g(\sigma_+)$ and $(g(\lambda\sigma_-) - g(\lambda\sigma_+)$ discussed earlier in this section (see Figures (10), (7), (8) and Eqs. (29) to (31)).

The comparison of the calculated pressures with the results of the computer simulation demonstrates again that the MSA-E, EXP and LEXP pressures are the most accurate ones. For small λ and strongly attractive potentials the EXP and LEXP pressures are more accurate than MSA-E, the latter tends to overestimate the pressure.

The fact that the MSA overestimates both U^* and P^* for small λ and large $1/T^*$ may be traced back to the behaviour of the pair correlation function

near $r = \lambda\sigma$. The MSA, i.e. $(g(\lambda\sigma_-) - g(\lambda\sigma_+)) \equiv \beta\varepsilon$ turns out to be inaccurate for small λ, the larger gap produced by the EXP and LEXP is certainly more accurate.

6 CONCLUSIONS

We have presented a critical evaluation of the optimized cluster theory, the optimized random phase approximation and of the mean spherical model for the example of a square-well fluid with a variable range of the attractive interaction. The investigation of the influence of the range of the interaction on the structure and the thermodynamic properties are particularly instructive. The results demonstrate that the OCT is definitely superior to the MSA, both in the accuracy of the predictions of the thermodynamic quantities and the pair correlation function in comparison to the computer experiment, and in its internal consistency. Earlier results for the special case of $\lambda = 1.5$[15] had indicated that the OCT thermodynamic properties are no better over all than the MSA results. Our work shows that this holds only for $\lambda = 1.5$ and is largely due—as had already been suspected—to a fortuitions concellation of errors. Our results for the square-well fluid supplement the results of Andersen *et al.*[4] for the Lennard–Jones fluid in establishing the accuracy of the OCT in describing the effect of attractive forces on the structure and thermodynamics of liquids.

Acknowledgements

This work has been supported by the Fonds zur Förderung der wissenschaftlichen Forschung in Österreich under project no. 3857.

References

1. W. H. Young, *Liquid Metals* 76, Ed. by R. Evans and D. A. Greenwood, Inst. of Physics Conf. Ser. Vol. **30**, 1 (1977).
2. J. Hafner, *Phys. Rev.*, **A15**, 617 (1977).
3. J. D. Weeks, D. Chandler, and H. C. Andersen, *J. Chem. Phys.*, **55**, 1497 (1971).
4. H. C. Andersen, D. Chandler, and J. D. Weeks, *Adv. Chem. Phys.*, **34**, 105 (1976).
5. R. Kumaravadivel and R. Evans, *J. Phys.*, **C9**, 3877 (1976).
6. G. Franz, W. Freyland, W. Gläser, F. Hensel, and E. Schneider, *J. Physique (Paris)*, **41**, C8-194 (1980).
7. V. K. Ratti and A. B. Bhatia, *Nuovo Cimento*, **B43**, 1 (1978).
8. J. M. Harder and M. Silbert, *Chem. Phys. Lett.*, **75**, 571 (1980).
9. J. Hafner, *J. Phys.*, **F6**, 1243 (1976).
10. H. C. Andersen and D. Chandler, *J. Chem. Phys.*, **53**, 547 (1970).
11. H. C. Andersen and D. Chandler, *J. Chem. Phys.*, **57**, 1918 (1972).
12. H. C. Andersen, D. Chandler, and J. D. Weeks, *J. Chem. Phys.*, **56**, 3812 (1972).
13. H. C. Andersen, D. Chandler, and J. D. Weeks, *J. Chem. Phys.*, **57**, 2626 (1972).

14. S. H. Sung, D. Chandler, and B. J. Alder, *J. Chem. Phys.*, **61**, 932 (1974).
15. W. R. Smith, D. Henderson, and Y. Tago, *J. Chem. Phys.*, **67**, 5308 (1977).
16. C. Regnaut, J. P. Badiali, and M. Dupont, *J. Physique (Paris)*, **41**, C8-603 (1980).
17. H. Beck and R. Oberle, *J. Physique (Paris)*, **41**, C8–289 (1980).
18. A. Rotenberg, *J. Chem. Phys.*, **43**, 1198 (1965).
19. F. Lado and W. W. Wood, *J. Chem. Phys.*, **49**, 4244 (1968).
20. D. Henderson, W. G. Madden, and D. D. Fitts, *J. Chem. Phys.*, **64**, 5026 (1976).
21. Y. Rosenfeld and R. Thieberger, *J. Chem. Phys.*, **63**, 1875 (1975).
22. T. Einwohner and B. J. Alder, *J. Chem. Phys.*, **49**, 1458 (1968).
23. B. J. Alder, D. A. Young, and M. A. Mark, *J. Chem. Phys.*, **56**, 3013 (1972).
24. Y. Tago, *J. Chem. Phys.*, **58**, 2096 (1973).
25. Y. Tago, *Phys. Lett.*, **A44**, 43 (1973).
26. Y. Tago, *J. Chem. Phys.*, **60**, 1528 (1974).
27. W. R. Smith, D. Henderson, and R. D. Murphy, *J. Chem. Phys.*, **61**, 2911 (1974).
28. D. D. Carley, *J. Chem. Phys.*, **67**, 1267 (1977).
29. D. D. Carley and A. C. Dotson, *Phys. Rev.*, **A23**, 1411 (1981).
30. J. A. Barker and D. Henderson, *Rev. Mod. Phys.*, **48**, 587 (1976).
31. E. Thiele, *J. Chem. Phys.*, **39**, 474 (1963).
32. M. S. Wertheim, *J. Math. Phys.*, **5**, 643 (1964).
33. L. Verlet and J. J. Weis, *Phys. Rev.*, **A5**, 939 (1972).
34. E. W. Grundke and D. Henderson, *Mol. Phys.*, **24**, 269 (1972).
35. W. Olivares and D. A. McQuarrie, *J. Chem. Phys.*, **65**, 3604 (1976).
36. C. Croxton, *Introduction to Liquid State-Physics*, Wiley (1974).
37. Y. Rosenfeld and N. W. Ashcroft, *Phys. Lett.*, **A73**, 31 (1979).
38. Y. Rosenfeld and N. W. Ashcroft, *Phys. Rev.*, **20A**, 1208 (1979).
39. R. Fletcher and M. J. D. Powell, *Comp. J.*, **6**, 163 (1963).
40. N. F. Carnahan and K. E. Starling, *J. Chem. Phys.*, **51**, 635 (1969).
41. L. Verlet and J. J. Weis, *Mol. Phys.*, **28**, 665 (1974).